Regular Schwarzschild black holes and cosmological models

Roberto Casadio[*]

Dipartimento di Fisica e Astronomia, Alma Mater Università di Bologna, 40126 Bologna, Italy, Istituto Nazionale di Fisica Nucleare, I.S. FLaG Sezione di Bologna, 40127 Bologna, Italy, and Alma Mater Research Center on Applied Mathematics (AM^2), Via Saragozza 8, 40123 Bologna, Italy

Alexander Kamenshchik[†]

Dipartimento di Fisica e Astronomia, Alma Mater Università di Bologna, 40126 Bologna, Italy and Istituto Nazionale di Fisica Nucleare, I.S. FLaG Sezione di Bologna, 40127 Bologna, Italy

Jorge Ovalle[‡]

Research Centre for Theoretical Physics and Astrophysics, Institute of Physics, Silesian University in Opava, CZ-746 01 Opava, Czech Republic and Sede Esmeralda, Universidad de Tarapaca, Avenida Luis Emilio Recabarren 2477, Iquique, Chile

(Received 5 February 2025; accepted 21 February 2025; published 11 March 2025)

We study regular Schwarzschild black holes in general relativity as an alternative to the singular counterpart. We analyze two types of solutions which are completely parametrized by the Arnowitt–Deser–Misner mass alone. We find that both families of regular solutions contain a de Sitter condensate at the core and admit (quasi) extremal black hole configurations in which the two horizons are arbitrarily close. Cosmological models based on these regular configurations are also analyzed, finding that they describe nontrivial Kantowski-Sachs universes free of singularities.

DOI: 10.1103/PhysRevD.111.064036

I. INTRODUCTION

It is well known that general relativity (GR) predicts singularities inside trapped regions, as stated in the singularity theorems [1,2], based on general and quite reasonable assumptions about the matter source. If we accept the weak cosmic censorship conjecture [3] to exclude the presence of naked singularities in nature, this means that the end of the collapse could well be described by vacuum black hole (BH) solutions of GR.

On the other hand, one can consider types of matter that circumvent the singularity theorems, allowing the collapse to form an event horizon without leading to a singularity. This is the case of regular (that is completely nonsingular) BHs. Unfortunately, this inevitably leads to the existence of at least a second horizon, the so-called Cauchy horizon, which has proven particularly problematic [4,5] (see also Refs. [6–15] for recent studies), thus motivating the strong cosmic censorship conjecture [3].

If we ignore for now all the problems associated with the Cauchy horizon and focus mainly on the construction and analysis of regular BHs, we will quickly realize that their production remains relatively easy (by employing still reasonable forms of matter). It is even possible to describe them in terms of a nonlinear electrodynamic theory [16]. Unfortunately, the above does not shed much light on the fundamental problem, i.e., the details of how the singularity is formed and, above all, how it is avoided. These are critical aspects in order to investigate the validity of GR under conditions of extreme curvature. If these nonsingular configurations really form during the collapse, effects associated with the Cauchy horizon seem to indicate that they are unstable, and would therefore represent at best a transitory state in the eventual formation of a singularity.

All the questions mentioned above require a detailed study of the inner BH region. Most cases exhibit a simple internal geometry, which is of course consistent with the ultimate state of the collapse. However, as argued in Ref. [17], the interior need not have this extreme simplicity, since the weak cosmic censorship conjecture establishes the formation of the event horizon before the singularity appears, thus allowing for more complex internal structures than the eventual final singularity. This is precisely the case reported in detail in Ref. [17], where alternative sources for the exterior region of the Schwarzschild BH in GR were investigated. Among the most attractive characteristics of these solutions, we highlight: (i) they depend on one parameter, namely, the total Arnowitt–Deser–Misner (ADM) mass $\mathcal{M}$ (no primary hair); (ii) no form of exotic matter is present; (iii) the space-time is continuous across the horizon

[*]Contact author: casadio@bo.infn.it
[†]Contact author: kamenshchik@bo.infn.it
[‡]Contact author: jorge.ovalle@physics.slu.cz

without additional structures on it (like a thin shell); (iv) tidal forces are finite everywhere for (integrable) singular solutions [14,18]; (v) there are simple regular solutions which might be an alternative to the Schwarzschild BH as the final stage of gravitational collapse.

So far, only singular cases of revisited Schwarzschild BHs have been considered, both in the cosmological context [19] and for the analytical modeling of the gravitational collapse [20]. The aim of this work is therefore twofold: first, to analyze in detail the case of regular Schwarzschild BHs and, second, to study the cosmological models associated with these solutions. The main difference is given by the unavoidable presence of an inner horizon which introduces new features with respect to the singular cases previously studied in Refs. [19,20]. About the first point, we will show that there exists (quasi) extremal configurations with Schwarzschild exterior, despite the metrics only depend on one parameter $\mathcal{M}$. For the second point, we are not aware of existing papers that exploit regular BH solutions to generate cosmological models. Again, the presence of two horizons makes the nonsingular cases richer than those corresponding to singular metrics that were studied in Ref. [19], leading to (quasi) cyclic evolutions.

II. INSIDE THE BLACK HOLE

We begin by reviewing briefly the approach employed in Ref. [19] for static and spherically symmetric metrics of the Kerr-Schild form [21]

$$ds^2 = -f(r)dt^2 + \frac{dr^2}{f(r)} + r^2 d\Omega^2, \tag{1}$$

where

$$f = 1 - \frac{2m(r)}{r}. \tag{2}$$

The Schwarzschild solution [22] is obtained by setting the Misner-Sharp-Hernandex mass function

$$m(r) = \mathcal{M}, \quad \text{for } r > 0, \tag{3}$$

where $\mathcal{M}$ is the ADM mass associated with a pointlike singularity at the center $r = 0$. The coordinate singularity at $r = 2\mathcal{M} \equiv h$ indicates the event horizon [23–27].

We slightly relax the condition (3) to[1]

$$m(r) = m(h) = h/2 = \mathcal{M}, \quad \text{for } r \geq h, \tag{4}$$

so that the metric function (2) is given by

$$f = \begin{cases} 1 - \frac{2m}{r} \equiv f^-, & \text{for } 0 < r \leq h \\ 1 - \frac{2\mathcal{M}}{r} \equiv f^+, & \text{for } r > h. \end{cases} \tag{5}$$

The system is governed by the Einstein-Hilbert action

$$S = \int \left(\frac{R}{2\kappa} + \mathcal{L}_{\rm M} \right) \sqrt{-g} d^4x, \tag{6}$$

with R the scalar curvature and the Lagrangian density $\mathcal{L}_{\rm M}$ representing ordinary matter. Equations (5) and (6) imply that $\mathcal{L}_{\rm M} = 0$ for $r > h$, and inside the horizon $0 < r < h$ one finds the energy-momentum tensor

$$T^\mu{}_\nu = \text{diag}[p_r, -\epsilon, p_\theta, p_\theta], \tag{7}$$

where the energy density ϵ, radial pressure p_r, and transverse pressure p_θ read[2]

$$\epsilon = \frac{2m'}{\kappa r^2}, \qquad p_r = -\frac{2m'}{\kappa r^2}, \qquad p_\theta = -\frac{m''}{\kappa r}, \tag{8}$$

where primes denote derivatives with respect to r. Since Eq. (8) are linear in the mass function m, any two solutions can be linearly combined, as a trivial case of gravitational decoupling [28,29].

From the contracted Bianchi identities $\nabla_\mu G^\mu{}_\nu = 0$ one obtains the continuity equation

$$\epsilon' = -\frac{2}{r}(p_\theta - p_r), \tag{9}$$

which implies that $p_\theta > p_r$ if the energy density ϵ decreases monotonically from the center outward ($\epsilon' < 0$). Continuity of the metric (5) across the horizon $r = h$ requires the matching conditions

$$m(h) = \mathcal{M}, \qquad m'(h) = 0, \tag{10}$$

and, from Eqs. (8) and (10), one must also have

$$\epsilon(h) = p_r(h) = 0. \tag{11}$$

The tension p_θ can instead be discontinuous across $r = h$.

III. REGULAR BLACK HOLES

In this section, we will analyze in detail the regular BHs with Schwarzschild exterior, starting with the scalar curvature for the interior metric (5), which reads

$$R = \frac{2rm'' + 4m'}{r^2}, \quad \text{for } 0 < r \leq h. \tag{12}$$

In order to have a regular BH solution, we start by assuming [17]

[1]We shall denote $F(h) \equiv F(r)|_{r=h}$ for any $F = F(r)$. We shall also use units with $c = 1$ and $\kappa = 8\pi G_{\rm N}$.

[2]Recall that the coordinates t and r exchange roles for $0 < r < h$.

$$R = \sum_{n=2}^{\infty} C_n r^{n-2}, \qquad n \in \mathbb{N}, \tag{13}$$

which, from Eq. (12), yields the mass function

$$m = M - \frac{Q^2}{2r} + \frac{1}{2}\sum_{n=2}^{\infty} \frac{C_n r^{n+1}}{(n+1)(n+2)}, \tag{14}$$

for $0 < r \leq h$, where M and Q are integration constants that can be identified with the ADM mass of the Schwarzschild solution and a charge for the Reissner-Nordström (RN) geometry, respectively. In order to have a nonsingular configuration, i.e., the Ricci scalar (12), Ricci square $R_{\mu\nu}R^{\mu\nu}$ and Kretschmann scalar $R_{\mu\nu\rho\sigma}R^{\mu\nu\rho\sigma}$ that are regular around $r = 0$, we must then impose

$$M = Q = 0. \tag{15}$$

On the other hand, Eq. (8) now yield

$$\kappa\epsilon = \sum_{n=2}^{\infty} \frac{C_n r^{n-2}}{n+2} = -\kappa p_r \tag{16}$$

and

$$\kappa p_\theta = -\frac{1}{2}\sum_{n=2}^{\infty} \frac{n}{n+2} C_n r^{n-2}, \tag{17}$$

for $0 < r \leq h$.

A. Regular Schwarzschild BHs

The simplest regular solution with Schwarzschild exterior was found by imposing the continuity conditions (10) on the mass function (14) [see Ref. [17] for all details], which yields

$$m = \frac{r}{2(n-2)}\left[(n+1)\frac{r^2}{h^2} - 3\left(\frac{r}{h}\right)^n\right], \tag{18}$$

where $2 < n \in \mathbb{N}$ is a parameter (not hair) which labels a family of regular BHs, and whose physical interpretation will be elucidated later. The corresponding metric function reads

$$f^- = 1 - \frac{1}{n-2}\left[n + 1 - 3\left(\frac{r}{h}\right)^{n-2}\right]\frac{r^2}{h^2}, \tag{19}$$

which gives rise to the curvature

$$R = \frac{n+1}{n-2}\left[4 - (n+2)\left(\frac{r}{h}\right)^{n-2}\right]\frac{3}{h^2}, \tag{20}$$

and is sourced by a fluid with

$$\kappa\epsilon = -\kappa p_r = \frac{n+1}{n-2}\left[1 - \left(\frac{r}{h}\right)^{n-2}\right]\frac{3}{h^2} \tag{21}$$

and

$$\kappa p_\theta = \frac{n+1}{n-2}\left[\frac{n}{2}\left(\frac{r}{h}\right)^{n-2} - 1\right]\frac{3}{h^2}, \tag{22}$$

with all expressions of course valid for $0 < r \leq h$. These fluids sourcing the BH solutions (19) satisfy the weak energy condition, and represent alternative sources for the Schwarzschild exterior $r > h$ in Eq. (5). Moreover, density and pressures behave monotonically, as we can see for $n = 4$ in Fig. 1.

We further notice that the region near $r = 0$ always behaves like the de Sitter solution with effective cosmological constant $\Lambda_{\text{eff}} = 3/h^2$, namely

$$f \sim 1 - r^2/h^2, \tag{23}$$

with

$$\kappa\epsilon = -\kappa p_r \sim -\kappa p_\theta \sim 3/h^2 \sim R/4. \tag{24}$$

For increasing $n \gg 2$, this de Sitter core grows toward the horizon, where the behavior changes in order to match the Schwarzschild exterior, as illustrated for $n = 30$ in Fig. 2.

B. Regular Schwarzschild BHs with $p_\theta(h) = 0$

We have seen that, unlike the density and radial pressure, the tension p_θ does not need to vanish on the horizon when the metric in the exterior is given by the Schwarzschild geometry. In fact, Eq. (22) yields a finite value $p_\theta \propto h^{-2}$ at $r = h$.

A family of regular solutions with smoother match with the outer Schwarzschild metric can be found by further imposing

$$p_\theta(h) \propto m''(h) = 0, \tag{25}$$

which yields

$$m = \frac{(n+1)(l+1)}{(n-2)(l-2)}\left[\left(\frac{r}{h}\right)^2 - \frac{3(l-2)}{(n+1)(l-n)}\left(\frac{r}{h}\right)^n + \frac{3(n-2)}{(l+1)(l-n)}\left(\frac{r}{h}\right)^l\right]\frac{r}{2}, \tag{26}$$

with $2 < n < l \in \mathbb{N}$. [Notice that Eq. (26) is invariant under the exchange $l \leftrightarrow n$.] The corresponding metric function reads

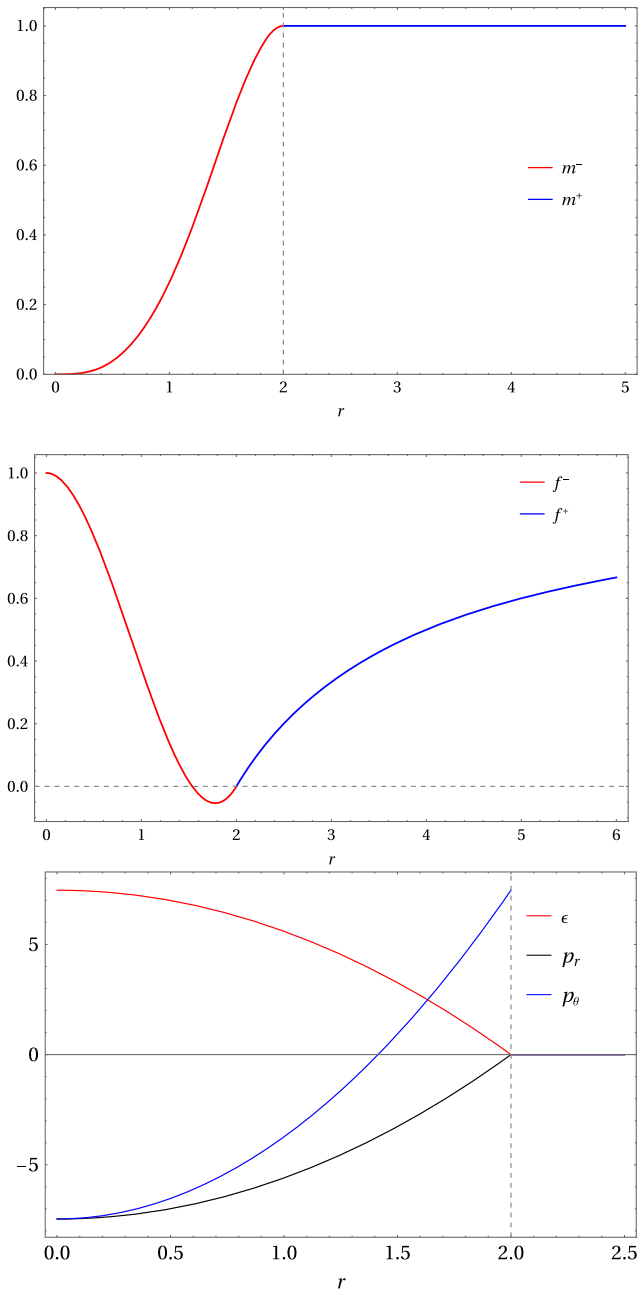

FIG. 1. Mass function (18) for $n = 4$ (top panel), corresponding metric function (5) (middle panel), and density and pressures (21) and (22) (rescaled by a factor of 100 for convenience; bottom panel). Vertical dashed lines represent the horizon $h = 2\mathcal{M}$. The Cauchy horizon is at $h_c = \sqrt{2/3}h$. (All quantities in units of $\mathcal{M}$).

$$f^- = 1 - \frac{(n+1)(l+1)}{(n-2)(l-2)}\left[\left(\frac{r}{h}\right)^2 - \frac{3(l-2)}{(n+1)(l-n)}\left(\frac{r}{h}\right)^n + \frac{3(n-2)}{(l+1)(l-n)}\left(\frac{r}{h}\right)^l\right], \tag{27}$$

and the source is characterized by

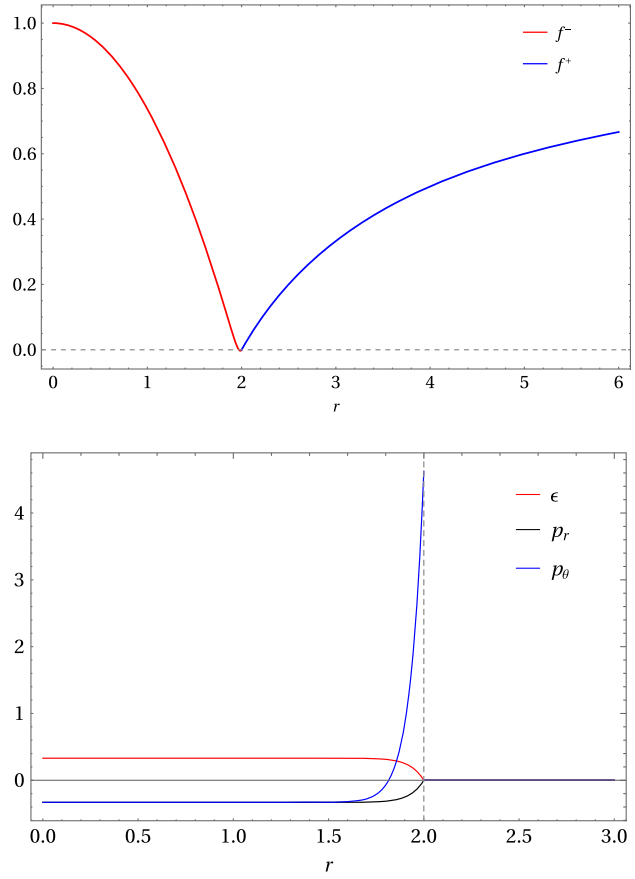

FIG. 2. Metric function (5) for $n = 30$ (upper panel), and corresponding density and pressures (21) and (22) (rescaled by a factor of 10 for convenience; lower panel). Vertical dashed line represents the horizon $h = 2\mathcal{M}$ coincident with the Cauchy horizon. (All quantities in units of $\mathcal{M}$).

$$\kappa\epsilon = \left[\left(\frac{r}{h}\right)^2 + \frac{n-2}{l-n}\left(\frac{r}{h}\right)^l - \frac{l-2}{l-n}\left(\frac{r}{h}\right)^n\right]\frac{3}{r^2} \times \frac{(n+1)(l+1)}{(n-2)(l-2)} = -\kappa p_r \tag{28}$$

and

$$\kappa p_\theta = -\left[\left(\frac{r}{h}\right)^2 + \frac{l(n-2)}{2(l-n)}\left(\frac{r}{h}\right)^l - \frac{n(l-2)}{2(l-n)}\left(\frac{r}{h}\right)^n\right]\frac{3}{r^2} \times \frac{(n+1)(l+1)}{(n-2)(l-2)}. \tag{29}$$

The above solution represents the simplest regular BH with Schwarzschild exterior having continuous energy-momentum tensor across the horizon, i.e., $T^\mu{}_\nu(h) = 0$.

Like the cases in Sec. III A, the solutions (27) satisfy the weak energy condition, and represent an alternative source for the Schwarzschild exterior $r > h$ in Eq. (5).

Moreover, the expressions (26)–(29) converge to those in Eqs. (18)–(22) for $l \gg n$ in the region $r < h$.

Equation (26) for $l = 4$ and $n = 3$ reads

$$m = \frac{r^3}{2h^4}\left(10h^2 - 15hr + 6r^2\right). \tag{30}$$

This is the same mass function for the metric found in semianalytic form in Ref. [30], which is however not of the Kerr-Schild type.[3] For a Kerr-Schild metric (1), the mass function (30) results in a Cauchy inner horizon at $r = h/2$ and the source is characterized by

$$\kappa\epsilon = -\kappa p_r = \frac{2}{r^2h^3}(h-r)^2(h+2r) \tag{31}$$

and

$$\kappa p_\theta = \frac{6}{h^3}(h-r), \tag{32}$$

with curvature

$$R = \frac{4}{r^2}\left(1 + \frac{5r^3}{h^3} - \frac{6r^2}{h^2}\right), \tag{33}$$

in the interior $0 < r \leq h$.

C. Extremal Schwarzschild BHs

It is easy to see that all of the regular BH interiors described by the metric functions (19) and (27) of the previous Sections have a single inner horizon. A rather interesting aspect of these solutions is then that they also contain configurations that are almost extreme black holes, as we will see below.

The interior metric function f^- has a minimum,

$$(f^-)'(r_e) = 0, \tag{34}$$

which, for the solutions (19), is located at

$$r_e = h\left[\frac{2}{3}\left(1 + \frac{1}{n}\right)\right]^{\frac{1}{n-2}}. \tag{35}$$

Since

$$\lim_{n\to\infty} r_e = h, \tag{36}$$

this minimum shifts toward the event horizon for increasing values of n. Consequently, the Cauchy horizon given by $f^-(h_c) = 0$, with $h_c < h$, is located at

$$h_c \sim h, \tag{37}$$

[3]To our knowledge, this was the first work about a BH with exact Schwarzschild exterior and distributed source.

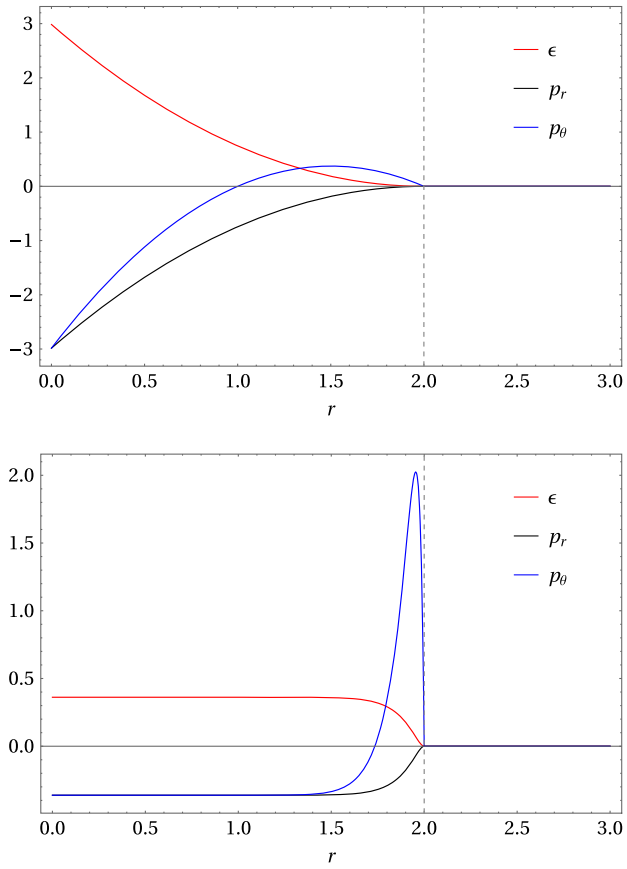

FIG. 3. Density and pressures (rescaled by a factor of 10 for convenience) for the solution (27) with $n = 3$ and $l = 4$ corresponding to the mass function (30) (upper panel), and the quasi-extremal case for $l = 4n = 80$ with the Cauchy and event horizon almost merging at $r = h$ (lower panel). Vertical dashed lines represent the horizon $h = 2\mathcal{M}$. (All quantities in units of $\mathcal{M}$).

for $n \gg 2$. Such configurations represent quasiextremal BHs with de Sitter core and Schwarzschild exterior separated by a (infinitesimally thin) region $h_c < r < h$, as displayed in Fig. 2. The parameter n for the solutions (19) therefore measures how close to extremality the object is.

Since the solutions (19) are a particular case of the expression in Eq. (27) for $l \gg n$, we conclude that the solutions (27) must have the same causal structure. It is still important to remark that the solutions (27) are generated by fluids whose energy-momentum tensor is completely continuous across the event horizon $r = h$, as displayed in Fig. 3. The solutions analyzed in Sec. III B can therefore be viewed as an improvement over those in Sec. III A.

We can obtain even smoother solutions by considering a generic polynomial of N terms of the form

$$m = C_3 r^3 + C_n r^n + C_l r^l + C_p r^p + \ldots, \tag{38}$$

where the unknown coefficients can be determined by the continuity condition (4) and

TABLE I. Interior of regular Schwarzschild BHs with mass functions (18) and (26).

$\{n,l\}$	$m(r)$	$\epsilon>0$	Energy condition
$\{2<n<l\}$	$m=\frac{(n+1)(l+1)}{(n-2)(l-2)}\left[\left(\frac{r}{h}\right)^2-\frac{3(l-2)}{(n+1)(l-n)}\left(\frac{r}{h}\right)^n+\frac{3(n-2)}{(l+1)(l-n)}\left(\frac{r}{h}\right)^l\right]\frac{r}{2}$	Yes	Weak
$\{2<n\ll l\}$	$m\sim\frac{r}{2(n-2)}\left[\frac{r^2}{h^2}(n+1)-3\left(\frac{r}{h}\right)^n\right]$	Yes	Weak
$\{2\ll n\ll l\}$	$m\sim\frac{r^3}{2h^2}$ Extremal BH with $h_c\sim h$	Yes	Weak
$\{2<n,l\to\infty\}$	$m=\frac{r}{2(n-2)}\left[\frac{r^2}{h^2}(n+1)-3\left(\frac{r}{h}\right)^n\right]$	Yes	Weak
$\{2\ll n,l\to\infty\}$	$m\sim\frac{r^3}{2h^2}$ Extremal BH with $h_c\sim h$	Yes	Weak

$$\frac{d^q m}{dr^q}(h)=0, \tag{39}$$

for all $1\le q\le N-1$. As we have seen, full continuity of the energy-momentum tensor across the horizon is obtained for $N=3$, corresponding to the inner metric functions (27). A summary of the cases with $N=3$ and $N=2$ is given in Table I for convenience. However, as we have just seen, the inner regular region could be much richer than illustrated in Table I.

IV. COSMOLOGY

For all the regular BHs described in Table I, the region $h_c<r<h$ lies between two horizons and can also be considered as a whole universe [31]. In fact, the metric signature is $(+,-,+,+)$ inside this region where r becomes a time coordinate. To make the role of time and spatial coordinates more explicit, we can swap $t\leftrightarrow r$ therein, so that the corresponding line element reads

$$ds^2=-\frac{dt^2}{F(t)}+F(t)dr^2+t^2d\Omega^2, \tag{40}$$

where

$$F=1-\frac{2m(t)}{t}\ge 0 \tag{41}$$

with the mass function m given by the different cases listed in Table I and $h_c\equiv t_1<t<t_0\equiv h$.

We can next write the metric (40) in terms of the cosmic (or synchronous) time defined by

$$d\tau=\pm\frac{dt}{\sqrt{F(t)}}, \tag{42}$$

which leads to the generic cosmological solution

$$ds^2=-d\tau^2+a^2(\tau)dr^2+b^2(\tau)d\Omega^2. \tag{43}$$

The metric (43) represents a Kantowski-Sachs homogeneous but anisotropic universe [32,33] with scale factors

$$a^2(\tau)\equiv F(\tau)$$
$$b^2(\tau)\equiv t^2(\tau). \tag{44}$$

The nonvanishing components of the corresponding Einstein tensor are given by

$$G_0^0=-\left(\frac{1}{b^2}+\frac{2\dot a\,\dot b}{ab}+\frac{\dot b^2}{b^2}\right) \tag{45}$$

$$G_1^1=-\left(\frac{1}{b^2}+\frac{2\ddot b}{b}+\frac{\dot b^2}{b^2}\right) \tag{46}$$

$$G_2^2=-\left(\frac{\dot a\,\dot b}{ab}+\frac{\ddot a}{a}+\frac{\ddot b}{b}\right), \tag{47}$$

where dots denote derivative with respect to τ.

Let us then consider a regular BH described in the first line of Table I, with $n=3$ and $l=4$, so that the function in Eq. (41) reads

$$F=6\left(\frac{t}{h}-1\right)\left(\frac{t}{h}-\frac{1}{2}\right)\left(\frac{t^2}{h^2}-\frac{t}{h}-\frac{1}{3}\right), \tag{48}$$

where t runs between the two horizons at $t=h$ and $t=h/2$. The corresponding expression for the cosmic time (42) is integrable, leading to a finite lapse between $t=h/2$ and $t=h$. If we choose the initial value $\tau=0$ corresponding to $t=h/2$, the final time can be computed numerically and is given by

$$\tau_0\equiv\tau(h)=\int_{1/2}^{1}\frac{dt}{\sqrt{F(t)}}\simeq 1.9h. \tag{49}$$

In the vicinity of the point $t=h/2$, we can write

$$t=\frac{h}{2}+y, \tag{50}$$

with $0\le y\ll h/2$, and we find

$$\tau\simeq 2\sqrt{\frac{h}{7}}\int_{\frac{h}{2}}^{\frac{h}{2}+y}\frac{dx}{\sqrt{x}}=4\sqrt{\frac{hy}{7}}. \tag{51}$$

Correspondingly, the components of the Kantowski-Sachs metric read

$$b^2 = t^2 \simeq \frac{h^2}{4}\left(1 + \frac{7\tau^2}{4h}\right), \tag{52}$$

and

$$a^2 = F \simeq \frac{49\tau^2}{64h^2}. \tag{53}$$

One can directly check that the scalar curvature

$$R = -\frac{\ddot{a}}{a} - 4\frac{\ddot{b}}{b} - 4\frac{\dot{a}\,\dot{b}}{ab} - 2\frac{\dot{b}^2}{b^2} - \frac{2}{b^2} \tag{54}$$

is regular near $\tau = 0$. Other invariants are also not singular and the universe is regular at $\tau = 0$.

We can repeat the analysis near $t = h$, by defining

$$t = h - y, \tag{55}$$

where again $0 \leq y \ll h/2$. The cosmic time then reads

$$\tau \simeq \tau_0 - 2\sqrt{hy}, \tag{56}$$

and the Kantowski-Sachs metric functions are given by

$$b^2 = t^2 \simeq h^2\left[1 - \frac{(\tau_0 - \tau)^2}{2h^2}\right] \tag{57}$$

and

$$a^2 = F \simeq \frac{(\tau_0 - \tau)^2}{4h^2}. \tag{58}$$

This point is also nonsingular.

Overall, the above case corresponds to a quasicyclic universe which starts at $\tau = 0$ with $a = 0$ and $b = h/2$ (the radius of the inner horizon). As the synchronous time increases, both a and b increase, but a reaches a maximum at $\tau = \tau_1$ determined by the condition

$$\frac{dF}{dt} = \frac{t}{h}\left(24\frac{t^2}{h^2} - 45\frac{t}{h} + 20\right) = 0, \tag{59}$$

after which a decreases and reaches zero at $\tau = \tau_0$, when $b = h$ (the radius of the outer horizon). It is easy to compute the solution of Eq. (59), which is given by

$$t_1 = \frac{45 - \sqrt{105}}{48}h \simeq 0.72h, \tag{60}$$

and the corresponding cosmic time can then be computed numerically, to wit

$$\tau_1 \simeq 0.79h. \tag{61}$$

Obviously, the first derivative of the scale factor b is always positive, since

$$\dot{b} = \dot{t} = \sqrt{F} = a. \tag{62}$$

Since $\ddot{b} = \dot{a}$, when the scale factor a is growing (for $0 < \tau < \tau_1$), the scale factor b grows with positive acceleration. For $\tau_1 < \tau < \tau_0$, the scale factor a is decreasing and the scale factor b increases with negative acceleration.

This behavior remains qualitative the same in all cases containing two horizons, the main difference being the location (or time) of the inner horizon (the outer horizon is fixed at $t = h$). For example, for $n = 3$ and $l = 0$, one finds

$$F = 3\left(1 - \frac{t}{h}\right)\left(\frac{t}{h} - \frac{1 + \sqrt{13}}{6}\right)\left(\frac{t}{h} - \frac{1 - \sqrt{13}}{6}\right), \tag{63}$$

and the inner horizon is at

$$t = \frac{1 + \sqrt{13}}{6}h \simeq 0.77h, \tag{64}$$

which is larger than the value $t = h/2$ for $n = 3$ and $l = 4$.

A particularly simple case is obtained for $n = 4$ and $l = 0$, namely

$$F = 3\left(1 - \frac{t^2}{h^2}\right)\left(\frac{t^2}{h^2} - \frac{2}{3}\right), \tag{65}$$

in which the coordinate time runs in the interval

$$0.82h \simeq \sqrt{\frac{2}{3}}h \leq t \leq h. \tag{66}$$

The function F for the three cases considered here is shown in Fig. 4. We finally remark that the sign of the proper time

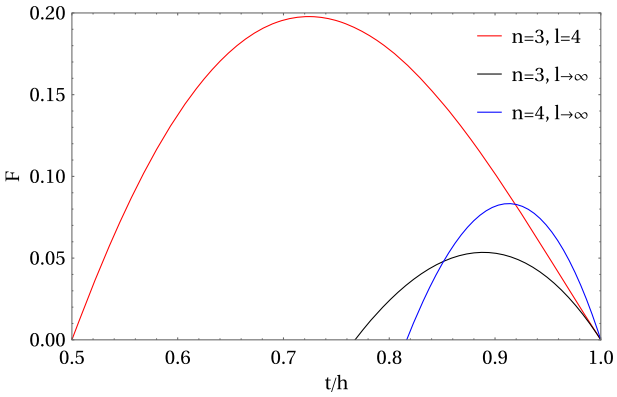

FIG. 4. Function F in Eq. (41) for the cases discussed in the main text.

τ can be inverted, according to the definition (42), so that the curves in Fig. 4 could be followed in either direction.

V. CONCLUSION

Circumventing the singularity theorem in GR necessarily implies the existence of nonclassical states of matter that somehow manage to stop the collapse. Regular configurations with finite energy density everywhere then always contain an additional inner horizon. Achieving this without introducing exotic matter and maintaining the Schwarzschild exterior is challenging. In this work, we obtained regular BHs sourced by a fluid that satisfies the weak energy condition and are characterized by a single charge, namely, the ADM mass $\mathcal{M}$ of the Schwarzschild exterior. Moreover, unlike the singular metrics considered previously in Refs. [19,20], these regular BHs admit (quasi) extremal configurations in which the two horizon (almost) coincide. At first glance, this might seem odd, since extremal configurations are usually achieved by specific combinations of at least two charges (e.g., electric charge $Q = \mathcal{M}$ for the Reissner-Nordström and angular momentum $a = \mathcal{M}$ for the Kerr solutions).

We remark that the solutions considered in this work technically admit quasiextremal configurations, since the two horizons are separated by a layer which can be made as thin as we want, thus effectively merging them in the limit of Eq. (36). In the same limit, the surface gravity $\kappa(r) = F'(r)$ on the Cauchy horizon also becomes as small as possible, namely

$$\lim_{n\to\infty} \kappa(h_c) = \lim_{n\to\infty} F'(h_c) = 0. \tag{67}$$

This fact is quite significant, and could have consequences in favor of the existence of stable regular BHs, since the instability caused by the mass inflation is precisely proportional to κ. This is a point that certainly deserves to be investigated further, since the existence of extremal BHs described only by the ADM mass $\mathcal{M}$, which also happen to be stable, would greatly support GR as the theory that correctly describes very compact objects.

We have also studied nonextremal configurations and showed that the layer between the two horizons describes anisotropic Kantowski-Sachs universes, which show a quasiperiodic evolution and contain no singularity at the end-points.

ACKNOWLEDGMENTS

R. C. and A. K. are partially supported by the INFN grant FLAG. The work of R. C. has also been carried out in the framework of activities of the National Group of Mathematical Physics (GNFM, INdAM). J. O. is partially supported by ANID FONDECYT Grant No. 1210041.

DATA AVAILABILITY

No data were created or analyzed in this study.

[1] R. Penrose, Phys. Rev. Lett. **14**, 57 (1965).
[2] S. W. Hawking and G. F. R. Ellis, *The Large Scale Structure of Space-Time*, Cambridge Monographs on Mathematical Physics (Cambridge University Press, Cambridge, England, 2011).
[3] R. Penrose, Riv. Nuovo Cimento **1**, 252 (1969).
[4] E. Poisson and W. Israel, Phys. Rev. Lett. **63**, 1663 (1989).
[5] E. Poisson and W. Israel, Phys. Rev. D **41**, 1796 (1990).
[6] A. Ori, Phys. Rev. Lett. **67**, 789 (1991).
[7] R. Carballo-Rubio, F. Di Filippo, S. Liberati, C. Pacilio, and M. Visser, J. High Energy Phys. 07 (2018) 023.
[8] A. Bonanno, A.-P. Khosravi, and F. Saueressig, Phys. Rev. D **103**, 124027 (2021).
[9] R. Carballo-Rubio, F. Di Filippo, S. Liberati, C. Pacilio, and M. Visser, J. High Energy Phys. 05 (2021) 132.
[10] R. Carballo-Rubio, F. Di Filippo, S. Liberati, C. Pacilio, and M. Visser, J. High Energy Phys. 09 (2022) 118.
[11] E. Franzin, S. Liberati, J. Mazza, and V. Vellucci, Phys. Rev. D **106**, 104060 (2022).
[12] R. Casadio, A. Giusti, and J. Ovalle, Phys. Rev. D **105**, 124026 (2022).
[13] A. Bonanno, A.-P. Khosravi, and F. Saueressig, Phys. Rev. D **107**, 024005 (2023).
[14] R. Casadio, A. Giusti, and J. Ovalle, J. High Energy Phys. 05 (2023) 118.
[15] J. Ovalle, Phys. Rev. D **107**, 104005 (2023).
[16] E. Ayon-Beato and A. Garcia, Phys. Rev. Lett. **80**, 5056 (1998).
[17] J. Ovalle, Phys. Rev. D **109**, 104032 (2024).
[18] V. N. Lukash and V. N. Strokov, Int. J. Mod. Phys. A **28**, 1350007 (2013).
[19] R. Casadio, A. Kamenshchik, and J. Ovalle, Phys. Rev. D **110**, 044001 (2024).
[20] S. Aoki and J. Ovalle, Phys. Rev. D **111**, 024037 (2025).
[21] R. P. Kerr and A. Schild, Proc. Symp. Appl. Math **17**, 199 (1965).
[22] K. Schwarzschild, Sitzungsber. Preuss. Akad. Wiss. Berlin (Math. Phys.) **1916**, 189 (1916), https://inspirehep.net/literature/3899.
[23] A. S. Eddington, Nature (London) **113**, 192 (1924).
[24] G. Lemaitre, Ann. Soc. Sci. Bruxelles A **53**, 51 (1933).
[25] D. Finkelstein, Phys. Rev. **110**, 965 (1958).
[26] M. D. Kruskal, Phys. Rev. **119**, 1743 (1960).

[27] G. Szekeres, Publ. Math. Debrecen **7**, 285 (1960), https://inspirehep.net/literature/44776.
[28] J. Ovalle, Phys. Rev. D **95**, 104019 (2017).
[29] J. Ovalle, Phys. Lett. B **788**, 213 (2019).
[30] M. Mars, M. M. Martín-Prats, and J. M. M. Senovilla, Classical Quantum Gravity **13**, L51 (1996).
[31] R. Doran, F. S. N. Lobo, and P. Crawford, Found. Phys. **38**, 160 (2008).
[32] R. Kantowski and R. K. Sachs, J. Math. Phys. (N.Y.) **7**, 443 (1966).
[33] R. W. Brehme, Am. J. Phys. **45**, 423 (1977).